Simulation of Airflow Patterns and Aerodynamic Forces on a Chambered Airfoil and Symmetric Airfoil with Maximum Thickness Variation

I Gede Kartana[1*], Anak Agung Adhi Suryanwan[1], I Gusti Ketut Sukadana[1]

[1]Mechanical Engineering Study Program, Faculty of Engineering, Universitas Udayana, Denpasar, Indonesia

A B S T R A C T

Flow across the airfoil can cause drag and lift forces. The difference in pressure between the top and bottom surfaces of the airfoil creates a force that is perpendicular to the flow of fluid, and this force is called the lift force, and parallel to the flow is called the drag force. The author conducted research on simulating airflow patterns across the airfoil with maximum thickness variations. In this research, the simulation method is CFD (Computational Fluid Dynamic) using ANSYS Fluent software. The solution or solver method used in this simulation is the SIMPLE (Semi Implicit Method for Pressure Linked Equation) scheme. The flow pattern is shown by the streamline formed on the symmetric airfoil for $\alpha=0°$, which will be symmetric, as well as the separation on the two sides, both the upper and lower sides. In contrast to the chambered airfoil, flow separation occurs only on the upper side. This indicates that there will be a pressure difference on the upper side and lower side so that the lift force can occur even though $\alpha=0°$, because the lower side shows the pressure side. The greater the maximum thickness, the faster flow separation occurs. Then the higher the velocity value, the flow separation will be delayed due to an increase in the momentum of the working fluid flow, which overcomes the shear stress that occurs. At the angle of attack $\alpha=0°$, the greater the maximum thickness of the chambered airfoil produces a greater lift force, while the symmetric airfoil does not produce lift.

1. Introduction

Aerodynamics is a basic science when discussing the principles of airplanes. One of the discussions in the science of aircraft aerodynamics is about the airfoil of the aircraft wing.[1,2] The phenomenon of airfoils, namely the presence of fluid movement that passes through an object, creates a problem in the design of moving industries, especially the fluid flowing in the airfoil. At the present time, the development of research using computing-based software is often encountered. This makes it easier for researchers in the calculation and simulation process, including the calculation process on the airfoil. One of the methods used in computing is the computational fluid dynamic (CFD) method. Many types of special software to

calculate fluid problems with the CFD method. All analysis software related to fluids uses the finite element method or Finite Volume, which is a calculation technique by dividing the domain area into cells or grids, which is also known as control volume. The governing equation is then discrete, and 3 is solved iteratively for each control volume. The result is an approximation of the value of each variable at a given point in the domain. Software that is often used in solving equations in CFD analysis includes Solidwork, Cosmoflow, GAMBIT, CATIA, ABAQUS, Pro Engineering, and ANSYS.[3-6]

The viscous effect is characterized by the presence of shear stress in the form of friction between the fluid and the solid surface both in internal flow and external

flow, the friction that will determine the physical state of the flow. Reynolds number is generally used to state that viscosity has an important role in determining the type/type of flow of a fluid. Furthermore, the flowing viscous fluid will form a boundary layer on the solid surface. This boundary layer becomes a hypothetical boundary which is the area of the dominant fluid viscosity effect and the area that can be considered an inviscid (non-viscous) region hypothetically.[7-10]

External flow across the interfering body will affect the flow phenomena that occur from the flow, such as the formation of wakes and drag forces caused by flow separation. Separation is indicated when the momentum of the working fluid upstream (upstream) is no longer able to overcome the shear stress that arises. As a result, the downstream momentum (downstream) will push a smaller momentum (upstream direction), and the flow will move in the opposite direction (towards the upstream). The phenomenon of This flow is called backflow/adverse pressure gradient occurs.[11-13]

Flow across the airfoil can cause drag and lift forces. The magnitude of the drag and lift forces is influenced by parameters, namely: coefficient of force, Flow Velocity, and outward flow projection. The coefficient of drag force and lift force is strongly influenced by the dimensions of the airfoil. Thus, the dimensions of the airfoil can affect the drag force and lift force that occurs.[14]

An airfoil is a form of aerodynamics intended to produce a large lift with the smallest possible drag. When an airfoil is passed by a fluid flow, the interaction between the airflow and the surface will cause variations in Velocity and pressure along the top and bottom surfaces of the airfoil as well as at the front and back of the airfoil. The difference in pressure between the top and bottom surfaces of the airfoil will cause a resultant force whose direction is perpendicular to the direction of the fluid flow, and this force is referred to as lift. The size of the lift that occurs will vary depending on the geometry of the airfoil and its operating conditions.[15,16] This study aims to simulate airflow patterns and aerodynamic forces on a chambered and symmetric airfoil with maximum thickness variation.
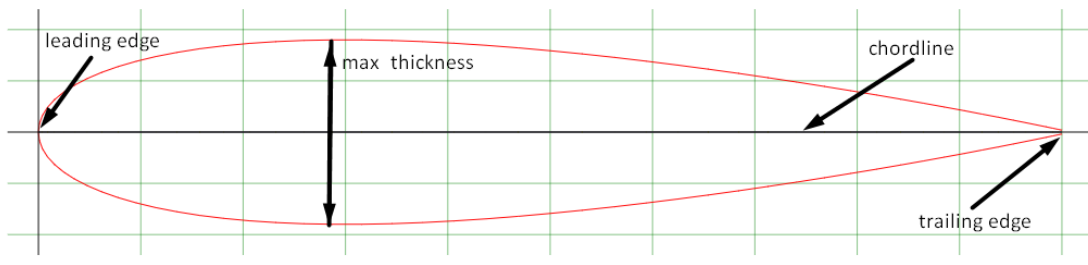
2. Methods

The research was conducted using the CFD (Computational Fluid Dynamic) simulation method using the ANSYS Fluent software. The following is an image of the simulated dimensions:
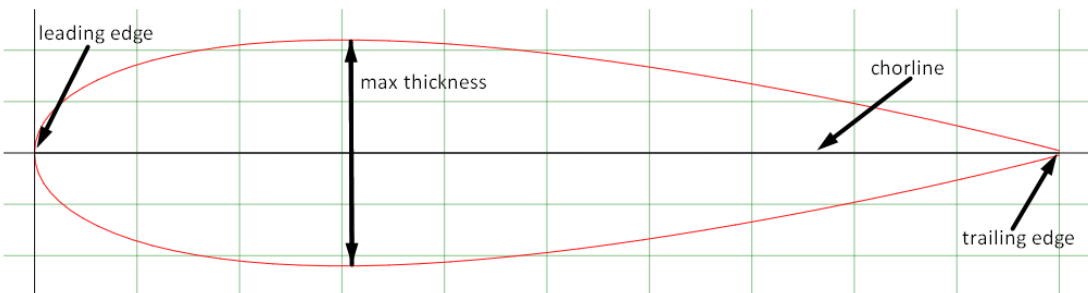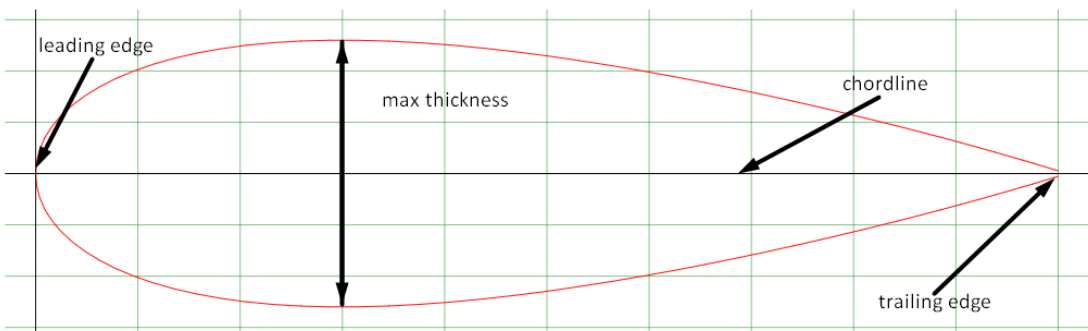

(a)

(b)
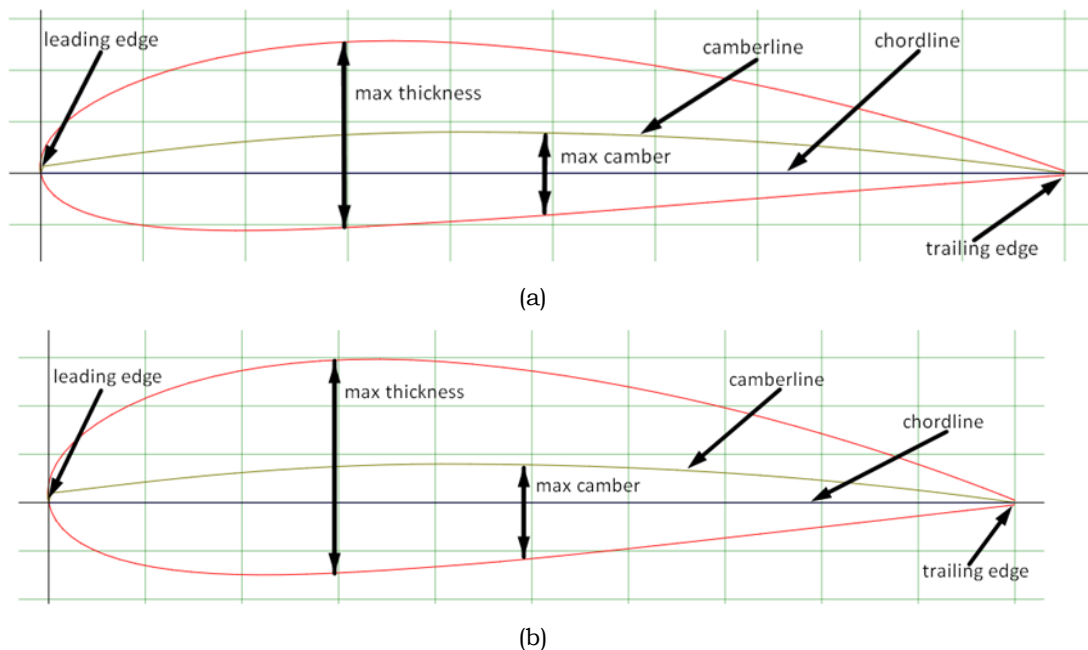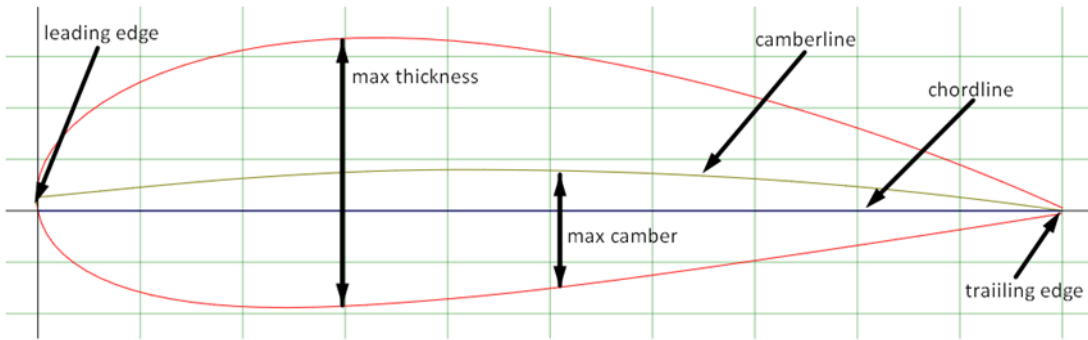
(c)

(d)

(e)

(f)

Figure 1. Airfoil to be simulated.

a. Airfoil has dimensions with a chord line length of 100 mm, a maximum thickness of 18 mm at a chord line of 29.2 mm, and a maximum chambered of 3.1 mm at a chord line length of 49.8 mm. b. Airfoil b has dimensions with a chord line length of 100 mm, a maximum thickness of 22 mm at a chord line length of 29.2 mm, and a maximum chambered of 2.9 mm at a chord line length of 49.8 mm. c. Airfoil c has dimensions with a chord line length of 100 mm, a maximum thickness of 26 mm at a chord line of 29.2 mm, and a maximum chambered of 2.7 mm at a chord line length of 52.8 mm. d. Airfoil has dimensions with a chord line length of 100 mm, a maximum thickness of 18 mm at a chord line of 28.7 mm, and a maximum chambered of 0 mm. e. Airfoil e has dimensions with a chord line length of 100 mm, a maximum thickness of 22 mm at a chord line length of 28.7mm, and a maximum chambered of 0 mm. f. Airfoil f has dimensions with a chord line length of 100 mm, a maximum thickness of 26 mm at a chord line length of 28.7 mm, and a maximum chambered of 0 mm.

Simulation of airflow phenomena in airfoils is carried out by importing geometries that have been made with Inventor software. Next is the meshing process. Based on the geometry that has been made, it can be determined the geometry as a cell cutting tool through the meshing process. The meshing process is also used to define meshing parameters for creating geometries. Meshing settings are made on the meshing properties and make geometric refinements. Meshing settings that need to be done include setting the division value. To refine the mesh, the next step will be the refinement process. Then, create a fluid domain by selecting the surface of the air inlet hole at the inlet (inflow) as the inlet pressure and the airflow outlet surface. The selected finite volume method is the segregated method, which is used to solve the mass, momentum, and energy conservation equations. With the segregated method, an equation for a particular variable is solved for all cells, then the equation for the next variable is solved for all cells, and so on. The solution or solver method used in this simulation is the SIMPLE (Semi Implicit Method for Pressure Linked Equation) scheme, which is a numerical procedure for solving the Navier-Stokes equation that uses the relationship between Velocity and pressure to obtain the mass conservation value and the pressure field value. The pressure equation is corrected to calculate a conservative flux set. The discretized momentum equation is solved implicitly, and the velocity correction is solved explicitly. The discretization method is done by choosing a divergency scheme for the momentum equation is linear upwind. This scheme is an interpolation method with explicit corrections based on local cell gradients. If the velocity value is negative, the solution to the equation is directed to the right, the left side is called upwind, and the right side is called downwind, and vice versa if the velocity value is positive. The k-omega turbulent model was chosen because it is numerically more stable, especially in its low Reynold number version, which tends to produce solutions that converge faster than the k-epsilon model, low Reynold number is more economical and elegant than the k-epsilon model for a high Reynold number. Low, which does not require the calculation of wall distance, addition of source term, or damping function based on friction velocity. Setting the time control time includes start time with a value of 0, time step: 1, and end time: enter the number of iterations of 1000 iterations. Furthermore, the simulation can be run with the run panel. The next process is post-processing, where the previously determined simulation results can be further processed to see the simulation results, either in the form of images or animations with certain color patterns.

3. Results and Discussion

The flow pattern of airfoil a with a speed of 80 m/s (Figure 2A), at the front of the airfoil (leading edge), the points stagnate at point (s) where the air velocity at point s is 0 m/s (stagnation) then experienced an increase in speed which was marked by green to reddish-yellow air velocity between 53 m/s to 88 m/s. After passing through the leading edge, the air velocity increases in the chambered airfoil, as indicated by the red area. In that area, the air velocity is around 94 m/s

to 106 m/s, and the air separation (sp) that occurs in this area can be seen. Indicated by a line separating red and yellow. The airflow then continues to the trailing edge area, wherein that area, the air again decreases in speed (increase in pressure), then a relatively small wake occurs, which is marked by a green color with an airspeed of around 47 m/s decreasing to a blue color at the end of the trailing edge. The pattern of airflow on airfoil a with a speed of 100 m/s (Figure 2B), at the front of the airfoil (leading edge), the points stagnate at point (s) where the air velocity at point s is 0 m/s (stagnation) increases Velocity marked with green to reddish-yellow air velocity ranges from 86 m/s to 103 m/s. After passing through the leading edge, the air velocity increases in the chambered airfoil, as indicated by the red area. In that area, the air velocity is at a speed of about 112 m/s to 121 m/s, and the air separation (sp) that occurs in this area can be seen. Indicated by a line separating red and yellow. The airflow then continues to the trailing edge area, wherein in that area, the air again experiences a decrease in speed (increase in

pressure). Then, a relatively small wake occurs, which is marked by a green color with an airspeed of about 51 m/s, decreasing to a blue color at the trailing edge. The pattern of airflow on airfoil a with a speed of 110 m/s (Figure 2C), at the front of the airfoil (leading edge), the points stagnate at point (s) where the air velocity at point s is 0 m/s (stagnation) increases Velocity marked with green to reddish-yellow air velocity is between 89 m/s to 112 m/s. After passing through the leading edge, the air velocity increases in the chambered airfoil, as indicated by the red area. In that area, the air velocity is around 130 m/s to 138 m/s, and it can be seen in the air separation (sp) that occurs in this area. Indicated by a line separating red and yellow. The airflow then continues to the trailing edge area, wherein that area, the air again experiences a decrease in speed (increase in pressure). Then a relatively small wake occurs, which is marked by a green color with an airspeed of about 73 m/s, decreasing to a blue color at the end of the trailing edge.
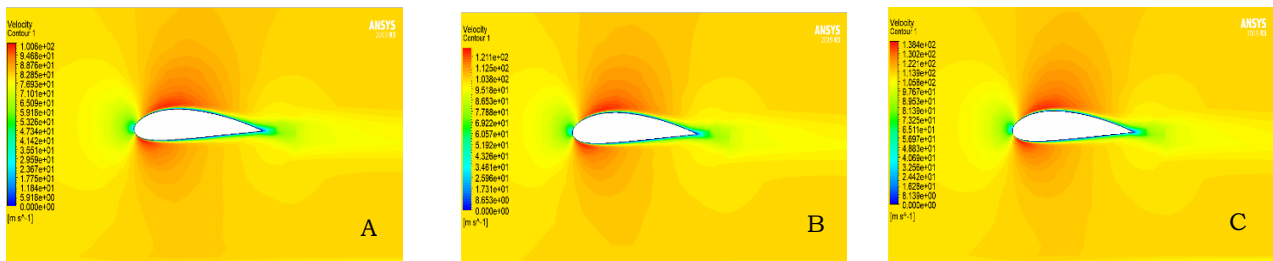

Figure 2. Airfoil a flow pattern with velocity 80, 100, 110 m/s.

Airfoil b flow pattern with 80 m/s velocities (Figure 3A) at the front of the airfoil (leading edge) stagnated points at the point (s) where the air velocity at that point s is 0 m/s (stagnation) the velocity increases which are indicated by a green to reddish-yellow color, and the air velocity is between 50 m/s to 94 m/s. After passing through the leading edge, the air velocity increases in the chambered airfoil, as indicated by the red area. In that area, the air velocity is around 100 m/s to 106 m/s, and the air separation (sp) that occurs in this area can be seen. Marked by a line that

separates red and yellow is known as the adverse pressure gradient. The mesh blockage phenomenon occurs as a result of the viscosity of the fluid. The airflow continues to the trailing edge area, wherein that area, the air again experiences a decrease in speed, which is indicated by a green to a blue color with an airspeed of around 47 m/s, decreasing to a speed of 6 m/s marked in blue at the end of the trailing edge. In the trailing edge area, the air velocity decreases due to the working fluid momentum to overcome the shear force or the effect of viscosity,

which is also characterized by the presence of a low-pressure area or wake. The flow pattern of airfoil b with a speed of 100 m/s (Figure 3B) at the front of the airfoil (leading edge) has a stagnation point at point (s) where the air velocity at point s is 0 m/s (stagnation) has a marked increase in speed with a green to reddish-yellow color, the air velocity is between 62 m/s to 117 m/s. After passing through the leading edge, the air velocity increases in the chambered airfoil, as indicated by the red area. In that area, the air velocity is around 125 m/s to 133 m/s, and it can be seen in the air separation (sp) that occurs in this area. Indicated by a line separating red and yellow. The airflow then continues to the trailing edge area, wherein in that area, the air again experiences a decrease in speed (increase in pressure). Then awake occurs, which is marked by a green to a blue color with an airspeed of about 62 m/s, decreasing to a speed of 7.8 m/s marked in blue at the trailing edge. In the trailing edge area, the air velocity decreases due to the momentum of the working fluid to overcome the shear force or the effect of viscosity which is also characterized by the presence of a low-pressure area

or time. The flow pattern of airfoil b with a speed of 110 m/s (Figure 3C) at the front of the airfoil (leading edge) experiences a stagnation of points at point (s) where the air velocity at point s is 0 m/s (stagnation) has a marked increase in speed with a green to reddish-yellow color, the air velocity is between 75 m/s to 122 m/s. After passing through the leading edge, the air velocity increases in the chambered airfoil, as indicated by the red area. In that area, the air velocity is at a speed of about 132 m/s to 141 m/s and can be seen in the air separation (sp) that occurs in this area. Indicated by a line separating red and yellow. The airflow then continues to the trailing edge area, wherein in that area, the air again experiences a decrease in speed (increase in pressure). Then awake occurs, which is marked by a green to a blue color with an airspeed of about 75 m/s, decreasing to a speed of 9.4 m/s marked in blue at the trailing edge. In the trailing edge area, the air velocity decreases due to the working fluid momentum to overcome the shear force or the effect of viscosity, which is also characterized by the presence of a low-pressure area or wake.
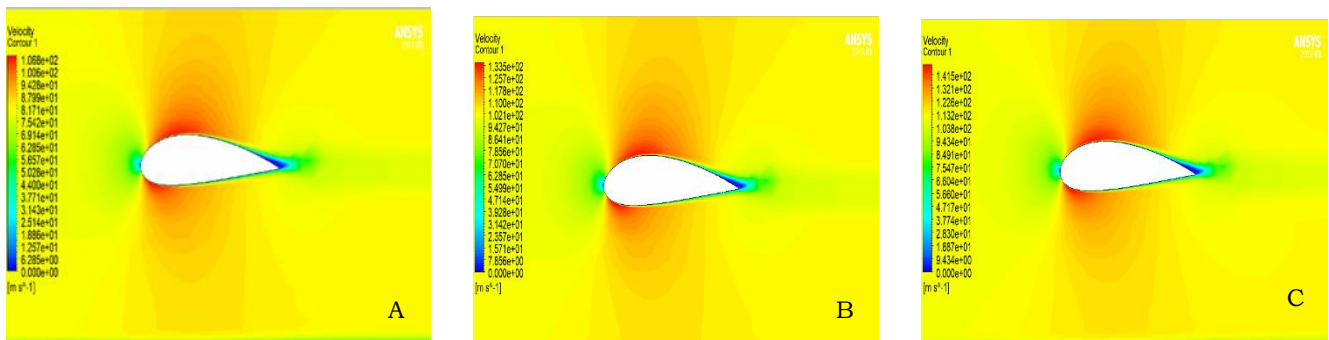

Figure 3. Airfoil b airflow pattern with speed 80,100, 110 m/s.

Airfoil c flow pattern with 80 m/s speed (Figure 4A), at the front of the airfoil (leading edge), the points stagnate at point (s) where the air velocity at the s point is 0 m/s (stagnation), and the velocity increases which are indicated by a green to reddish-yellow color, the air velocity is between 51 m/s to 90 m/s. After passing through the leading edge, the air velocity increases in the chambered airfoil, indicated by the red area. In that area, the air velocity is around 96 m/s to 109 m/s, and the air separation (sp) that occurs in this

area can be seen. Indicated by a line separating red and yellow. The airflow then continues to the trailing edge area, wherein in that area, the air again experiences a decrease in speed (increase in pressure). Then there is a very visible wake marked by green to a blue color with an airspeed of about 45 m/s, decreasing to a speed of 6.4 m/s, marked in blue at the trailing edge. In the trailing edge area, the air velocity decreases, resulting in an increase in turbulence due to changes in speed. The flow pattern

of airfoil c with a speed of 100 m/s (Figure 4B) at the front of the airfoil (leading edge) has a stagnation point at point (s) where the air velocity at point s is 0 m/s (stagnation) has a marked increase in speed with green to reddish-yellow air velocities between 64 m/s to 120 m/s. After passing through the leading edge, the air velocity increases in the chambered airfoil, as indicated by the red area. In that area, the air velocity is around 129 m/s to 137 m/s, and the air separation (sp) that occurs in this area can be seen. Indicated by a line separating red and yellow. The airflow then continues to the trailing edge area, wherein in that area, the air again experiences a decrease in speed (increase in pressure). Then there is a very visible wake marked by a green to a blue color with an airspeed of about 56 m/s, decreasing to a speed of 8 m/s marked in blue at the trailing edge. In the trailing edge area, the air velocity decreases, resulting in an increase in turbulence due to changes in speed. The flow pattern of airfoil c with a speed of 110 m/s (Figure 4C) at the front of the airfoil (leading edge) experiences a stagnation of points at point (s) where the air velocity at point s is 0 m/s (stagnation) has a marked increase in speed with a green to reddish-yellow color, the air velocity is between 71 m/s to 124 m/s. After passing through the leading edge, the air velocity increases in the chambered airfoil, as indicated by the red area. In that area, the air velocity is around 133 m/s to 150 m/s, and the air separation (sp) that occurs in this area can be seen. Indicated by a line separating red and yellow. The airflow then continues to the trailing edge area, wherein in that area, the air again experiences a decrease in speed (increase in pressure). Then there is a very visible wake marked by a green to a blue color with an airspeed of about 62 m/s decreasing to a speed of 8.8 m/s s are, marked in blue at the trailing edge. In the trailing edge area, the air velocity decreases, resulting in an increase in turbulence due to changes in speed.
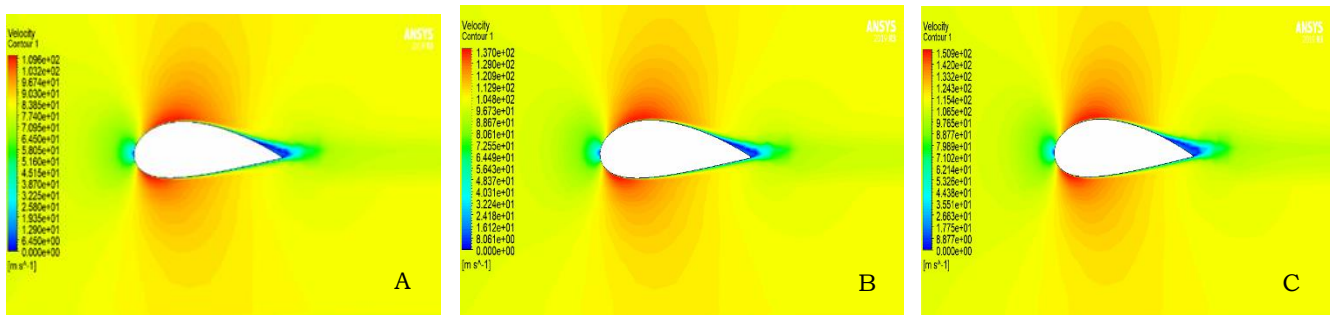

Figure 4. Airfoil c flow pattern with speeds 80,100, 110 m/s.

Airfoil d flow pattern with 80 m/s speed (Figure 5A) on the front of the airfoil (leading edge) stagnated at point (s) where the air velocity at point s is 0 m/s (stagnation) has an increase in speed which is indicated by green to reddish-yellow air velocity between 52 m/s to 87 m/s. After passing through the leading edge, the air velocity increases in the chambered airfoil, as indicated by the red area. In that area, the air velocity is around 93 m/s to 99 m/s, and it can be seen in the air separation (sp) that occurs in this area. Indicated by a line separating red and yellow. The airflow then continues to the trailing edge area, wherein that area, the air again experiences a decrease in speed (increase in pressure), then a relatively small wake occurs, which is marked by a green color with an airspeed of about 41 m/s decreasing to a blue color with a speed of about 6 m /s at the trailing edge. The flow pattern of airfoil d with a speed of 100 m/s (Figure 5B) at the front of the airfoil (leading edge) has a stagnation point at point (s) where the air velocity at point s is 0 m/s (stagnation) has a marked increase in Velocity with a green to reddish-yellow color, the air velocity is between 65 m/s to 102 m/s. After passing through the leading edge, the air velocity increases in the chambered airfoil, as indicated by the red area. In that area, the air velocity

is around 109 m/s to 124 m/s, and the air separation (sp) that occurs in this area can be seen. Indicated by a line separating red and yellow. The airflow then continues to the trailing edge area, wherein that area, the air again experiences a decrease in speed (increase in pressure), then a relatively small wake occurs, which is marked by a green color with an airspeed of about 58 m/s decreasing to a blue color with a speed of about 7.3 m/s at the trailing edge. The flow pattern of airfoil d with a speed of 110 m/s (Figure 5C) at the front of the airfoil (leading edge) has a stagnation point at point (s) where the air velocity at point s is 0 m/s (stagnation) has a marked increase in Velocity with a green to reddish-yellow color, the air velocity is

between 80 m/s to 112 m/s. After passing through the leading edge, the air velocity increases in the chambered airfoil, as indicated by the red area. In that area, the air velocity is at a speed of about 120 m/s to 137 m/s, and can be seen in the air separation (sp) that occurs in this area. Indicated by a line separating red and yellow. The airflow then continues to the trailing edge area wherein that area, the air again experiences a decrease in speed (increase in pressure) then a relatively small wake occurs, which is marked by a green color with an airspeed of about 56 m/s decreasing to a blue color with a speed of about 8 m/s. s at the trailing edge.
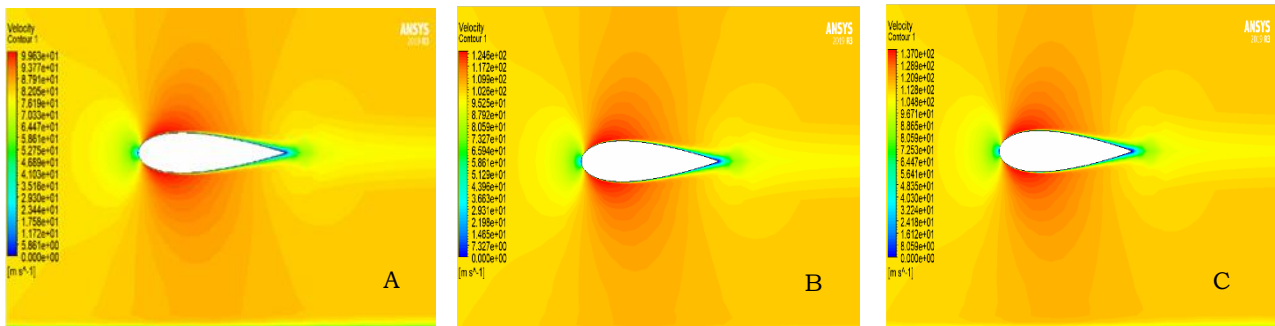

Figure 5. Airfoil d airflow pattern at 80,100, 110 m/s.

Airfoil e flow pattern with 80 m/s speed (Figure 6A) at the front of the airfoil (leading edge) stagnated at point (s) where the air velocity at point s is 0 m/s (stagnation) with an increase in speed which is indicated by a green to reddish-yellow color. The air velocity is between 54 m/s to 91 m/s. After passing through the leading edge, the air velocity increases in the chambered airfoil, as indicated by the red area. In that area, the air velocity is around 97 m/s to 103 m/s, and it can be seen in the air separation (sp) that occurs in this area. Indicated by a line separating red and yellow. The airflow then continues to the trailing edge area, wherein that area, the air again experiences a decrease in speed (increase in pressure), then a relatively visible wake occurs, which is marked by a green color with an airspeed of about 48 m/s decreasing to a blue color with a speed of about 6 m/s s at the trailing edge. The flow pattern of the airfoil e

with a speed of 100 m/s (Figure 6B) at the front of the airfoil (leading edge) experiences a stagnation of points at point (s) where the air velocity at point s is 0 m/s (stagnation) which is marked by an increase in Velocity. With a green to reddish-yellow color, the air velocity is between 68 m/s to 114 m/s. After passing through the leading edge, the air velocity increases in the chambered airfoil, as indicated by the red area. In that area, the air velocity is at a speed of about 122 m/s to 129 m/s, and it can be seen in the air separation (sp) that occurs in this area. Indicated by a line separating red and yellow. The airflow then continues to the trailing edge area, wherein in that area, the air again experiences a decrease in speed (increase in pressure). Then a relatively visible wake occurs, which is marked by a green color with an airspeed of about 53 m/s, decreasing to a blue color with a speed of about 7.6 m/s at the trailing edge. The

flow pattern of airfoil e with a speed of 110 m/s (Figure 6C) at the front of the airfoil (leading edge) experiences a stagnation of points at point (s) where the air velocity at point s is 0 m/s (stagnation) has a marked increase in speed with a green to reddish-yellow color, the air velocity is between 75 m/s to 126 m/s. After passing through the leading edge, the air velocity increases in the chambered airfoil, as indicated by the red area. In that area, the air velocity is around 134 m/s to 142 m/s, and it can be seen in the air separation (sp) that occurs in this area. Indicated by a line separating red and yellow. The airflow then continues to the trailing edge area, wherein that area, the air again experiences a decrease in speed (increase in pressure), then a relatively small wake occurs, which is marked by a green color with an airspeed of about 50 m/s decreasing to a blue color with a speed of about 8.3 m/s at the trailing edge.
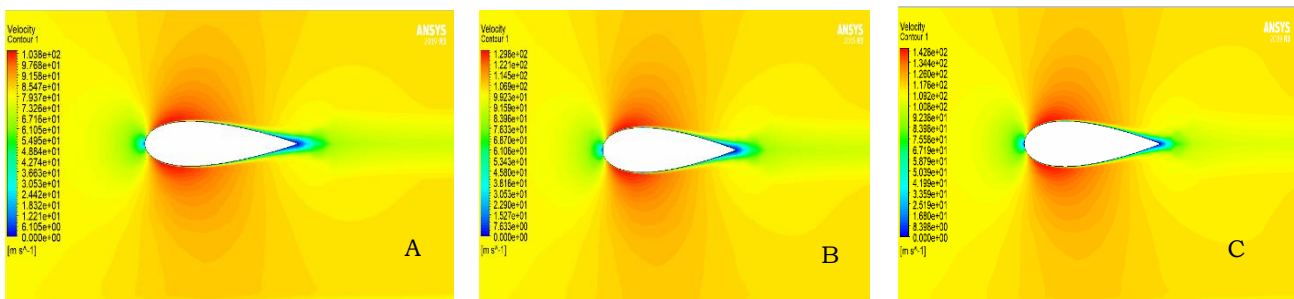

Figure 6. Airfoil e flow pattern with velocity 80,100, 110 m/s.

Airfoil f flow pattern with a velocity 80 m/s (Figure 7A) at the front of the airfoil (leading edge) stagnated at point (s) where the air velocity at point s is 0 m/s (stagnation) has an increase in speed which is indicated by a green to reddish-yellow color, the air velocity is between 56 m/s to 94 m/s. After passing through the leading edge, the air velocity increases in the chambered airfoil, as indicated by the red area. In that area, the air velocity is around 100 m/s to 107 m/s, and the air separation (sp) that occurs in this area can be seen. Indicated by a line separating red and yellow. The airflow then continues to the trailing edge area, wherein that area, the air again experiences a decrease in speed (increase in pressure). Then a relatively visible wake occurs, which is marked by a green color with an airspeed of about 50 m/s, decreasing to a blue color with a speed of about 6.3 m/s at the trailing edge. The airfoil flow pattern f with a speed of 100 m/s (Figure 7B) at the front of the airfoil (leading edge) has a stagnation point at point (s) where the air velocity at point s is 0 m/s (stagnation) has a marked increase in speed with a green to reddish-yellow color, the air velocity is between 70 m/s to 110 m/s. After passing through the leading edge, the air velocity increases in the chambered airfoil, as indicated by the red area. In that area, the air velocity is around 118 m/s to 134 m/s, and the air separation (sp) that occurs in this area can be seen. Indicated by a line separating red and yellow. The airflow then continues to the trailing edge area, wherein that area, the air again experiences a decrease in speed (increase in pressure), then a relatively visible wake occurs, which is marked by a green color with an airspeed of about 63 m/s decreasing to a blue color with a speed of about 7.8 m/s at the trailing edge. The flow pattern of the airfoil f with a speed of 110 m/s (Figure 7C) at the front of the airfoil (leading edge) has a stagnation point at point (s) where the air velocity at point s is 0 m/s (stagnation) has a marked increase in speed with a green to reddish-yellow color, the air velocity is between 78 m/s to 121 m/s. After passing through the leading edge, the air velocity increases in the chambered airfoil, as indicated by the red area. In that area, the air velocity is at a speed of about 130 m/s to 147 m/s, and the air separation (sp) that occurs in this area can be seen. Indicated by a line separating red

and yellow. The airflow then continues to the trailing edge area, wherein that area, the air again experiences a decrease in speed (increase in pressure). Then a relatively visible wake occurs, which is marked by a green color with an airspeed of about 69 m/s, decreasing to a blue color with a speed of about 8.6 m/s at the trailing edge.
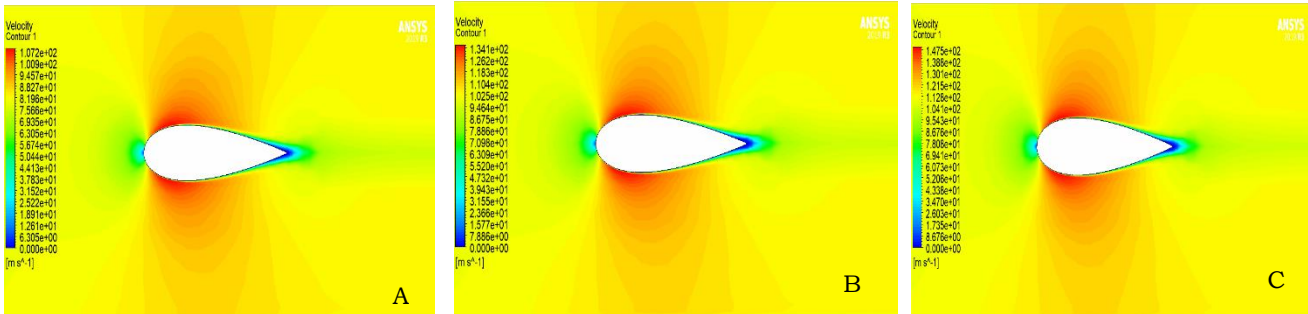

Figure 7. Airfoil airflow pattern f velocity 80,100, 110 m/s.

Table 1. Airfoil velocity and force data chambered.

No	Airfoil	Speed (m/s)	Drag force (N)	Lift force (N)	Coefficient drag	Coefficient lift
1	Airfoil a	80	0.07834418	0.19140993	0.12790887	0.31250599
		100	0.11876773	0.31279644	0.1939065	0.51068807
		110	0.14182872	0.38351864	0.23155709	0.62615287
2.	Airfoil b	80	1.1679324	2.5290873	1.9068284	4.1291223
		100	1.6655959	3.7979932	2.7193401	6.2008052
		110	1.9932213	4.631443	3.2542388	7.5615396
3	Airfoil c	80	1.331646	1.7562394	2.1741159	2.8673296
		100	2.0285089	2.8396449	3.3118513	4.6361547
		110	2.4316173	3.0884342	3.9699874	5.0423417

Table 2. Symmetric airfoil speed & force data.

Airfoil	Speed (m/s)	Drag force (N)	Lift force (N)	Coefficient drag	Coefficient lift
Airfoil d	80	0.75738001	0	1.2365388	0
	100	1.141201	0	1.8631853	0
	110	1.3616296	0	2.2230687	0
Airfoil e	80	0.96072656	0	1.5685332	0
	100	1.4544189	0	2.3745613	0
	110	1.7180283	0	2.804944	0
Airfoil f	80	1.2099496	0	1.9754279	0
	100	1.8181911	0	2.9684751	0
	110	2.173564	0	3.5486758	0

In symmetric airfoils, the style of the elevator will eliminae each other on the upper side and lower side. In contrast, the drag force will increase with the increasing speed and contact area of the working fluid, $F_D = \frac{1}{2} . p . V^2 . S . C_D$ means that the greater the maximum thickness, the greater the contact area.

4. Conclusion

The greater the maximum thickness, the faster the flow separation occurs. The flow pattern is indicated by the streamline that is formed on the symmetric airfoil for $\alpha = 0°$, which will be symmetric a well as the separation on the two sides, both on the upper side and lower side. In contrast to the chambered airfoil, flow separation occurs only on the upper side. Then the higher the velocity value, the flow separation will be delayed due to an increase in the momentum of the working fluid flow which overcomes the shear stress that occurs. At the angle of attack $\alpha = 0°$, the greater the maximum thickness of the chambered airfoil produces a greater lift force as well as the drag force, while symmetric airfoils do not produce lift. At the angle of attack $\alpha = 0°$, the greater the maximum thickness of the chambered airfoil produces a larger lift coefficient as well as the drag coefficient, while symmetric airfoils do not produce a lift coefficient because symmetric airfoils do not produce lift force.

5.References

1. Anderson JD. Computational fluid dynamics: The basic with application. 2nd ed. McGraw-Hill: New York. 1995.

2. Shams TA, Shah SIA, Javed A, Hamdani SHR. Airfoil selection procedure, wind tunnel experimentation and implementation of 6DOF modeling on a flying wing micro aerial. Micromachines (Basel). 2020; 11(6): 553.

3. Bronz M, Condomines JP, Hattenberger G. Development of an 18 cm micro air vehicle: Quark. ENAC; Toulouse, France: 2013.

4. Spoery MT. Wong K. Proceedings of the 9th Annual International Aerospace Congress, School of Aerospace, Mechanical and Mechatronic Engineering. University of Sydney; Sydney, Australia: 2001. Design and development of a micro air vehicle (µav) concept: Project Bidule.

5. Bronz M, Hattenberger G, Moschetta JM. Development of a long endurance mini-uav: Eternity. Int J Micro Air Veh. 2013; 5: 261-72.

6. Petricca L, Ohlckers P, Grinde C. Micro-and nano-air vehicles: State of the art. Int J Aerosp Eng. 2011; 2011: 214549.

7. McLain TW, Beard RW, Barber DB, Knoebel NB. An overview of MAV research at Brigham Young University. NATO; Brussels, Belgium: 2007.

8. Cai G, Dias J, Seneviratne L. A survey of small-scale unmanned aerial vehicles: Recent advances and future development trends. Unmanned System. 2014; 2:175-99.

9. Embacher M, Fasel HF. Direct numerical simulations of laminar separation bubbles: investigation of absolute instability and active flow control of transition to turbulence. J Fluid Mech. 2014; 747:141-85.

10. Cosyn P, Vierendeels J. Design of fixed wing micro air vehicles. Aeronaut J. 2007; 111: 315-26.

11. Spedding G, McArthur J. Span efficiencies of wings at low Reynolds numbers. J Aircr. 2010; 47: 120–128.

12. Ananda G, Sukumar P, Selig MS. Measured aerodynamic characteristics of wings at low Reynolds numbers. Aerosp Sci Technol. 2015; 42: 392-406.

13. Stevens BL, Lewis FL, Johnson EN. Aircraft control and simulation: dynamics, controls design, and autonomous systems. John Wiley & Sons; Hoboken, NJ, USA: 2015.

14. De Tavernier D, Baldacchino D, Ferreira C. An integral boundary layer engineering model for vortex generators implemented in XFOIL. Wind Energy. 2018; 21: 906-21.

15. Coder JG, Maughmer MD. Numerical validation of the Squire–Young formula for profile-drag prediction. J Aircr. 2015; 52: 948-55.

16. Morgado J, Vizinho R, Silvestre M, Páscoa J. XFOIL vs. CFD performance predictions for high lift low Reynolds number airfoils. Aerosp Sci Technol. 2016; 52: 207-14.